ACS NANO
Cite This: ACS Nano XXXX, XXX, XXX–XXX
www.acsnano.org

ARTICLE

Directed Assembly of Au-Tipped 1D Inorganic Nanostructures *via* Nanolithographic Docking

Avichai Marcovici,[†,§] Guillaume Le Saux,[†,§] Viraj Bhingardive,[†,§] Pazit Rukenstein,[‡,§] Kobi Flomin,[‡,§] Karam Shreteh,[‡,§] Roxana Golan,[§] Taleb Mokari,[*,‡,§] and Mark Schvartzman[*,†,§]

[†]Department of Materials Engineering, [‡]Department of Chemistry, and [§]Ilse Katz Institute for Nanoscale Science and Technology, Ben-Gurion University of the Negev, Beer-Sheva, 8410501, Israel

Supporting Information

ABSTRACT: **Controlled assembly of nanostructures is a key challenge in nanotechnology. In this work, we introduce an approach for the controlled assembly of 1D nanodumbbells—Au-tipped semiconductor nanorods—into arbitrary 2D higher architectures, by their chemical docking to nanopatterned functionalities. We realized the docking functionalities *via* nanoimprinted metallic nanodots functionalized with an organic monolayer, whose terminal thiol groups chemically bind the nanodumbbell tips. We demonstrated that the functional nanopattern encodes the nanodumbbell assembly and can be designed to deterministically position nanodumbbells in two possible modes. In the single-docking mode, the nanodot arrays are designed with a spacing that exceeds the nanodumbbell length, restricting each nanodumbbell to dock with one edge and physically connect with its free edge to one of the neighboring nanodumbbells. Alternatively, in the double-docking mode, the nanodots are spaced to exactly fit the nanodumbbell length, allowing nanodumbbell docking with both edges. We found that the docking kinetics can be described by a random attachment model, and verified that for the used docking chemistry, nanodumbbells that are docked to the same dot do not interact with each other. Our work demonstrates the possibility for massively parallel positioning of sub-100 nm 1D semiconductor nanostructures, and can potentially enable their future integration into functional nanodevices and nanosystems.**

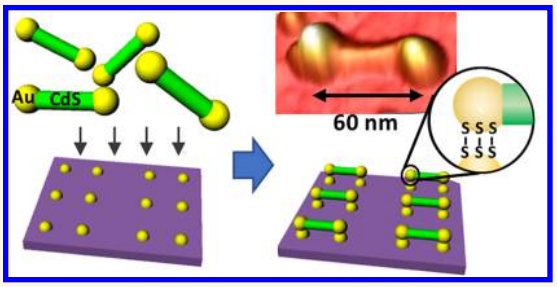

KEYWORDS: *nanodumbbells, nanoimprint, directed assembly, surface functionalization, bottom-up*

One-dimensional nanostructures, such as nanowires and nanorods, have been attracting a great deal of interest in the nanoresearch community as building blocks for functional devices and systems in many applications including electronics,[1] light emitting,[2] lasing,[3] and photovoltaics.[4] These nanostructures can be synthesized with a size, shape, and composition that can be controlled at the atomic level.[5,6] Furthermore, they can be designed with electronic configurations and unique physical properties, *e.g.*, ballistic conductivity,[7] making them perfect candidates for quantum electronics. However, the difficulty in spatially manipulating such miniature objects has constituted a major obstacle toward practical applications. Self-assembly offers an autonomous organization of building blocks at a variety of size scales;[8] however it is driven to reach the lowest energetic state against a decreased entropy, and thus cannot produce arbitrary geometries and long-range order required for functional devices and systems. Therefore, 1D nanostructures cannot be integrated into functional nanosystems by self-assembly alone, but must be guided by a top-down fabricated platform that determines their position.

During the last two decades, various guiding platforms have been proposed. Microfluidic-based assemblies, for example, can place nanowires with an accuracy of a few micrometers.[9] Contact printing[10] or nanocombing[11] was shown to control the nanowire position, but only in one coordinate. Dielectrophoretic organization could presumably reach nanometer accuracy upon the miniaturization of dielectrophoretic electrodes,[12] but such electrodes could complicate the fabrication of a nanowire circuit. Surface-guided growth from a nanopatterned catalyst can position nanowires with the accuracy of (±)50 nm, yet it also misplaces a significant part of them by hundreds of nanometers, probably due to catalyst migration during the high-temperature growth process.[13,14] Besides the limited positioning accuracy, these methods have been restricted so far to nanowires grown by chemical vapor deposition, whose diameter is tens of nanometers and above and whose length is usually in the tens of micrometers. Conversely, directed assembly of nanostructures with sub-10 nm dimensions, such as liquid phase synthesized nanorods,[15,16] still remains a challenge. This challenge is mostly associated with the fact that

Received: June 12, 2018
Accepted: September 25, 2018
Published: September 25, 2018

DOI: 10.1021/acsnano.8b04443
ACS Nano XXXX, XXX, XXX–XXX

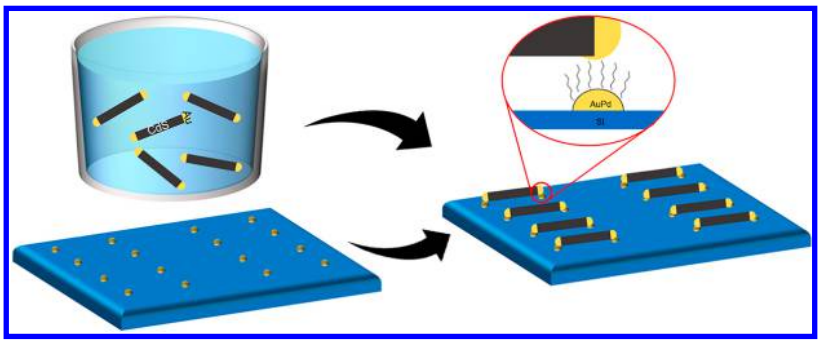

Figure 1. Schematic illustration of "docking" quasi-1D nanostructures to miniaturized surface functionalities.

the features that guide such an assembly must be the same size as the nanorods themselves, *i.e.*, at a sub-10 nm scale.

Discrete 1D nanostructures can, in principle, be positioned in a massively parallel manner with nanometer accuracy by anchoring to miniaturized surface functionalities. An obvious advantage of this approach, when compared to state-of-the-art methods, is that its positioning precision is determined by the size of the docking functionalities. Today, surface features sized below 5 nm can be nanopatterned by a variety of methods including electron-beam,[17] nanoimprint,[18] or block copolymer micelle lithography.[19] Recently, assembly directed by chemical anchoring to nanopatterned functionalities has been demonstrated for carbon-based 1D nanomaterials, including thiolated DNA origami attached to nanopatterned Au nanodots through covalent bonding[20] and carboxyl-terminated carbon nanotubes attached to amine-functionalized nanodots.[21] On the contrary, anchoring-based assembly of inorganic 1D nanostructures has not been demonstrated up until now. In particular, anchoring of inorganic nanostructures is challenged by the difficulty to bind the nanostructures to the nanofunctionalities exclusively *via* their edges.

Fourteen years ago, one of the coauthors (T.M.) reported the synthesis of metal-tipped semiconductor nanorods, which were called nanodumbbells.[22] One of the main motivations of that work was the formation of natural anchoring points that could serve as recognition elements for directed self-assembly. Since then, site-selective growth has been demonstrated for different material compositions, such as PtNi and PtCo tips on CdS nanorods,[23] Ag and PbS tips on CdS nanorods,[24] and ZnTe tips on ZnSe nanorods.[25] Furthermore, selective growth of metal tips was also demonstrated on nanostructures with other shapes, such as tetrapods.[26] However, the concept of a directed assembly of these nanostructures *via* chemically grown metallic anchors has not been realized so far.

In this work, we demonstrate the directed assembly of inorganic nanodumbbells *via* "chemical docking". The docking functionalities consisted of controllably positioned sub-10 nm metallic dots coated with organic monolayers terminated *ad hoc* to anchor the nanodumbbell tips (Figure 1). The docking itself was achieved then by attaching the nanodumbbell tips to the functionalized nanodots through covalently bonding their moieties to both surfaces. We demonstrated that through the docking we can deterministically configure nanodumbbells into arbitrary 2D arrays, whose architecture is encoded by the nanodot pattern. This approach of the programmed organization of inorganic quasi-1D nanostructures can potentially facilitate their parallel integration into functional nanodevices and systems, whose nanoscale dimensions as well as the structural and functional complexity are unachievable today.

RESULTS AND DISCUSSIONS

We prepared Au−CdS−Au nanodumbbells according to a previously published method.[27] Briefly, we first synthesized CdS nanorods, whose length was varied between 40 and 60 nm by controlling the reaction time. Then, Au tips sized between 1 to 3 nm were selectively grown on the nanorod edges (Figure 2a). Detailed information about the nanodumbbell synthesis is provided in the Materials and Methods section and the Supporting Information.

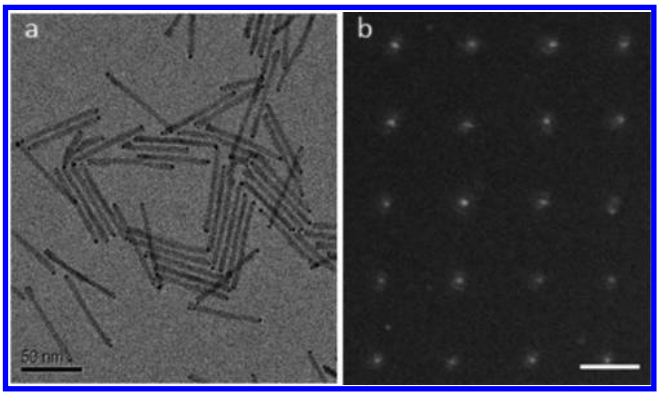

Figure 2. (a) Transmission electron microscopy image of Au−CdS−Au nanodumbbells. (b) Scanning electron microscopy micrograph of nanopatterned docking arrays. Scale bars are 50 nm.

In this work, nanoimprint lithography was used to produce docking arrays. Nanoimprint offers a clear advantage for this application due to the unique combination of (i) ultrasmall (down to a few nm) feature size,[28] (ii) high throughput and scalability,[29] and (iii) pattern arbitrariness. Electron-beam lithography can be used to produce miniaturized metallic features for anchoring nanosized objects;[30] however, it is a serial, low-throughput, and expensive method, which is unsuitable for realistic applications. On the other hand, block copolymer micelle lithography can be used to produce docking nanoarrays in a scalable manner,[31] but it can produce only uniform hexagonal arrays.[19] Here, we used a process previously reported by us, which included nanoimprint lithography and pattern transfer based on an angle evaporated mask, resist etching, metal deposition, and lift off.[32] We obtained nanodots that were typically 10−15 nm in size and, by thermal annealing, further miniaturized them to sub-5 nm dimensions.[32] Notably, this fabrication approach was previously used to produce nanodot arrays for the selective binding of distinct nano-objects, such as DNA,[20] carbon nanotubes,[21] and transmembrane protein in cells.[33,34]

DOI: 10.1021/acsnano.8b04443
ACS Nano XXXX, XXX, XXX−XXX

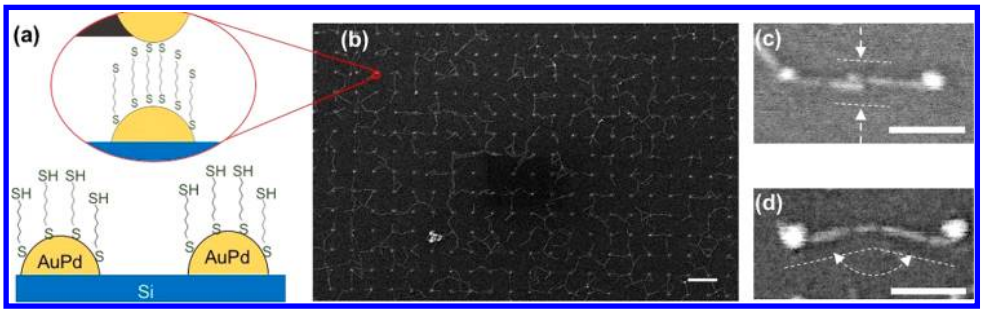

Figure 3. (a) Scheme of a dithiol self-assembled monolayer on AuPd nanodots. (b) Typical assembly result of nanodumbbells on a thiolated nanodot array. Scale bar is 150 nm. (c) Two docked nanodumbbells connected side-by-side. (e) Two docked nanodumbbells connected with their edges. Scale bar for (c) and (e) is 50 nm.

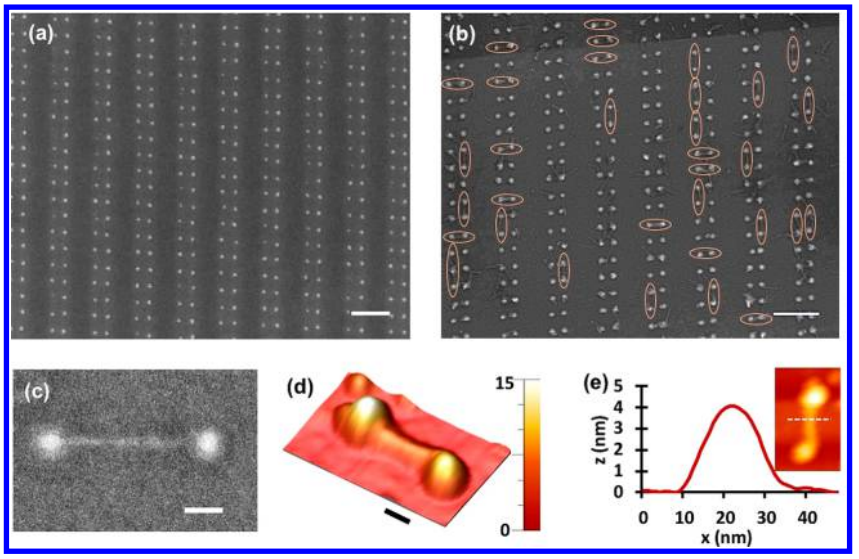

Figure 4. SEM images of (a) nanodot array arranged in pairs and (b) docked nanodumbbells on the same array, with double-docking events circled (right). Scale bars are 200 nm. (c) High-resolution SEM of a nanodumbbell anchored by double docking. Scale bar is 20 nm. (d) High-resolution AFM of a nanodumbbell anchored by double docking. Scale bar is 20 nm. (e) AFM profile of the docked nanodumbbell that confirms that the nanodumbbell lays on the surface.

Our arbitrarily patterned dot arrays encode the assembly of nanodumbbells into any desirable higher architecture. Figure 2b shows a 2D array of sub-10 nm AuPd nanodots. The spacing between the dots is 60 nm, matching the nanodumbbell length. Such an array was designed for the programmable assembly of nanodumbbells into a continuous grid. We chose AuPd as the material for docking nanodots since it can be easily functionalized with thiol and has a very small grain size (typically a few nanometers), making this alloy ideal for the nanofabrication of sub-20 nm features.[35]

Since both Au nanodumbbell tips and AuPd docking nanodots can chemisorb thiols, our natural choice for the docking chemistry was based on dithiols (Figure 3a). To this end, we first coated AuPd nanodots with 1,6-hexanedithiol (see Materials and Methods), which chemisorbs on the surface through one thiol and forms a closely packed self-assembled monolayer (SAM).[36] In this case, the outer thiol group will be available for the docking of nanodumbbells (Figure 3a).

The assembly of the nanodumbbells onto the docking arrays was carried out by immersing the functionalized substrates (see Materials and Methods) into a toluene-based solution of freshly synthesized nanodumbbells. Figure 3b presents a scanning electron miscroscopy (SEM) image of a typical assembly of nanodumbbells on arrays of nanodot arrays with edge-to-edge separation between of about 100 nm, a bit less than twice the nanodumbbell length. It is clearly seen that all the nanodumbbells are selectively docked through their tips to the functionalized nanodots. Notably, this scenario, at which the nanodots' spacing exceeds the nanodumbbell length, precludes double docking, *i.e.*, binding one nanodumbbell to a pair of nanodots with both its edges. Indeed, here the nanodumbbells docked to the nanodots with one edge only, *i.e.*, formed single-docking-based assembly.

In addition to the typical single-docking described above, many neighboring nanodumbbells connected to each other with their free edges. Using high-resolution close-up SEM, we detected two different types of such a connection: (i) side-by-side parallel connection (Figure 3c) and (ii) end-to-end connection at an angle determined by the nanorod length and nanodot spacing (Figure 3d). Interestingly, both types of connection were reported previously in the context of nanorod self-assembly. Specifically, nanorods form a parallel side-by-side connection when their self-assembly is regulated by antiparallel coupling between permanent dipole moments along the rod axis[37,38] or van der Waals forces.[39] Alternatively, nanorods form an end-to-end connection when their self-assembly is kinetically limited or regulated by solvent evaporation, in which localized high nanorod concentration

DOI: 10.1021/acsnano.8b04443
ACS Nano XXXX, XXX, XXX−XXX

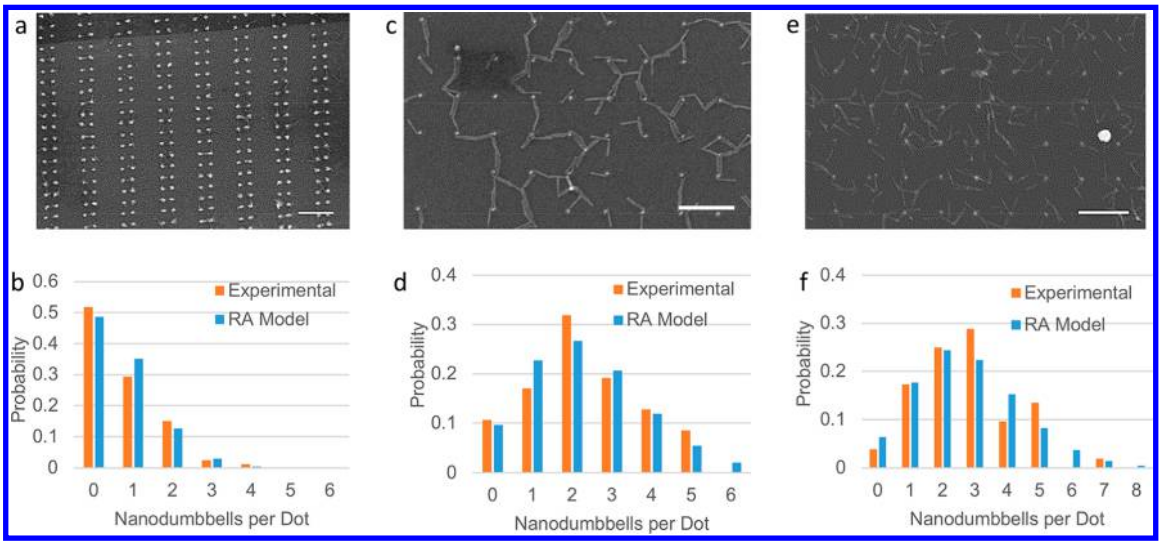

Figure 5. SEM micrographs of various docking experiments (a, c, e) and associated docking probability for each experiment, with random attachment model for comparison (b, d, f).

promotes the nanorod clustering.[40] Here, we experimentally observed both connections in docked nanodumbbells, for which one edge was fixed at the docking nanodots (Figure 3c and d). This phenomenon is particularly interesting, since the docking was done using relatively short molecules that are expected to restrict or limit the mobility of the docked nanodumbbells. Yet, it seems that the nanodumbbells that initially docked at a random orientation could still freely rotate around the point of docking and finally stick to each other. We speculate that some existing Au−thiol bonds break and new Au−thiol bonds form simultaneously, allowing the nanodumbbells to rotate while keeping their edge docked.[41]

Thanks to the complete arbitrariness of the nanofabricated docking pattern, we could also create conditions at which distinct nanodumbbells are controllably docked with both their edges. For this purpose, we arranged docking nanodots in pairs (Figure 4a), with a spacing that matches the nanodumbbell length. Figure 4b shows a typical array of docked nanodumbbells, where more than 20% of the docking is done with both of their edges to the neighboring nanodots. Figure 4c and d show high-resolution SEM and atomic force microscopy (AFM) of a nanodumbbell attached by double docking to a pair of nanodots. The AFM profile (Figure 4e) shows that the height of the nanodumbbell in the center is 4 nm, which is equal to the nanodumbbell diameter. This measurement confirms that the nanodumbbells, while chemically attached to the nanodots, lay on the surface and are not suspended. For a given bulk concentration of 250 nM nanodumbbells (see Supporting Information for the estimation of concentration), we probed different assembly times, from 24 to 96 h, and found no significant difference in the occurrence of the double docking. On the basis of this finding, we presume that most of the docking events occurred within the early stages of the assembly process. Interestingly, we found that the nanodumbbell docking is irreversible. To that end, we immersed the substrates with docked nanodumbbells into solvents with various polarity, including toluene, water, and water with soap, for a few hours and found that the immersion did not affect the nanodumbbell positioning. We explain this docking irreversibility by stable and strong thiol−gold covalent bonds that connect between the dots and nanodumbbell tips, as well as by van der Waals forces formed between the nanodumbbells and the substrate surface. Notably, we presume the existence of such van der Waals forces based by the fact that the docked nanodumbbells are in direct contact with the surface, as follows from the AFM measurements (Figure 4e).

It should be mentioned that in this work inorganic quasi-1D nanostructures with sub-10 nm width were precisely positioned in a parallel manner. Notably, nanodumbbell self-assembly onto pairs of nanoelectrodes was previously reported by Sheldon *et al.*[42] Yet, this self-assembly was not guided by chemical functionalities, and therefore was not site-specific. Furthermore, the width of the electrodes used in that work was sized at 100 nm scale, precluding nanodumbbell positioning with nanometer accuracy. Finally, electron beam lithography used to pattern electrodes is a serial fabrication method, which is suitable for prototyping rather than for scalable fabrication in realistic applications. On the contrary, here we demonstrate a combination of (i) chemically guided assembly to ensure high specificity of nanodumbbell positioning, (ii) sub-10 nm docking functionalities to ensure nanometer precision in the nanodumbbell positioning, and (iii) fabrication of docking features by nanoimprint lithography, a parallel and scalable nanopatterning technique.

Directed assembly of individual nanodumbbells is important for many applications. Still, docking of multiple nanodumbbells to the same vacancy site was often observed. It is worth noting that the number of nanodumbbells available for docking was always substantially larger than the number of vacant docking sites. On the other hand, a significant reduction in the nanodumbbell concentration could produce many unoccupied docking vacancies. Therefore, understanding the docking kinetics is essential to obtain a well-controlled assembly, thus achieving the highest possible yield of docked nanodumbbells and concurrently minimizing their multiple docking. To analyze the docking kinetics, we used a simplified balls-in-boxes model[31] based on the following assumptions: (a) for any closed system, there is a finite number of nanodumbbells and docking sites, (b) the model counts only the nanodumbbells docked to the nanodots and assumes that those were the only assembled nanodumbbells, (c) the docking is random, *i.e.*, a nanodumbbell can dock to any vacancy (*i.e.*, docking

DOI: 10.1021/acsnano.8b04443
ACS Nano XXXX, XXX, XXX−XXX

functionality) with the same probability, and (d) multiple dockings to the vacancy are defined as independent events, *i.e.*, the probability that a nanodumbbell would dock to a certain vacancy does not depend on how many nanodumbbells have been already docked to that vacancy.

In this case, the probability of one vacancy to link A nanodumbbells is given by

$$P = \frac{\binom{D}{A}(N-1)^{D-A}}{N^D} \quad (1)$$

where D and N are the total number of nanodumbbells and docking sites, respectively (see Supporting Information for the detailed model).

We analyzed a few arrays of docked nanodumbbells and probed different nanodot arrangements, as well as different bulk concentrations of nanodumbbells ranging from 10 nM to 2.5 μM (see Supporting Information for the estimation of the concentration). In each case, we calculated the experimental probability $P(A)$ by counting how many vacancies (*i.e.*, docking dots) are connected to A nanodumbbells and dividing this number by the total number of vacancies (Figure 5). We also calculated the theoretical probability for each A based on eq 1.

Comparison between the modeled and experimental probabilities shows that they greatly fit regardless of the pattern geometry and the total number of docked nanodumbbells. This finding confirms that the nanodumbbells are distributed between the docking sites in a random manner. Furthermore, the nearly perfect fit between the modeled and experimental probabilities proves that for the tested systems the nanodumbbells were docked in statistically independent events. Based on the fit between the model and experimental observation, we conclude that the nanodumbbells docked to the same nanodot do not interact with each other in a way that prevents multiple docking, at least when the number of nanodumbbells attaching to each dot is below the maximum observed here (*i.e.*, 7). Interestingly, the data presented in Figure 5a and b include nanodumbbells assembled by single docking and double-docking events; all were counted in the calculations. Specifically, each individual attachment of the nanodumbbell tip to a nanodot was counted as one single docking event whether the second nanodumbbell tip is docked or not. Still, we obtained the same good fit between the theoretical and experimental probabilities as was observed for assemblies on the patterns that allow only single docking (Figure 5c–f).

It should be noted that the docking described here is most probably regulated by the kinetics of the reaction between the terminal thiol groups and the Au nanodumbbell tips. Thus, we assume that for a long enough assembly time the number of nanodumbbells at each dot would increase to the level at which they prevent additional nanodumbbells from docking due to steric hindrance. In this case, the number of nanodumbbells at each nanodot is expected to be saturated and more uniformly distributed among the nanodots. Notably, another possible way bind nanodumbbells to nanodots is by biotin–avidin conjugation, previously shown to connect nanodumbbells to each other.[43] Here, we demonstrated that biotin–avidin binding can also be used to dock nanodumbbells to nanodots (see Supporting Information and Figure S4). Yet, due to the extremely low dissociation rate of the biotin–avidin bond (7.5×10^{-8} s^{-1}),[44] such a binding will also be irreversible and thus kinetically regulated. A possible way to achieve a more uniform distribution is by creating an assembly system governed by thermodynamics and not by kinetics. Recently, controlled binding of nanoparticles,[30] carbon nanotubes,[21] and DNA origami[45] to lithographically patterned functionalities was demonstrated using DNA hybridization. There, the formed double DNA had a melting point close to room temperature, ensuring that the controlled assembly reached thermodynamic equilibrium. In the near future, we intend to explore DNA hybridization as an alternative to thiol–Au binding for obtaining thermodynamically controlled nanodumbbell docking.

We assume that the number of docked nanodumbbells can be limited to a certain extent by miniaturizing the docking nanodots, so that steric hindrance would prevent multiple nanodumbbell attachment. Such steric hindrance was previously demonstrated for site-selective attachment of individual nanoparticles.[30,46] We presume that a similar self-limitation based on steric hindrance can be achieved by producing nanodots with a similar or smaller size than that of the nanodumbbell tips. Fabrication of features with sizes of a few nanometers is possible by several advanced lithographic methods, such as electron-beam[47] or nanoimprint lithography,[32] but is still extremely challenging. In addition, extremely small docking nanodots will require very narrow distribution of the nanodumbbell length. Figure S3 schematically shows a nanodumbbell with a length l_n and a tip diameter d_n, which is docked to a pair of nanodots with a diameter d_d and center-to-center separation l_d. For the ideal double-docking (Figure S3a), the dots and the tips overlap with their centers, so $l_d = l_n + d_n$. The shortest possible nanodumbbell for the double docking is shown in Figure S3b, for which $l_n(\min) = l_d - d_d - 2d_n$. On the other hand, the longest nanodumbbell to allow double docking is shown in Figure S3c, for which $l_n(\max) = l_d + d_d$. The size of the nanodumbbell tips d_n is ~2 nm on average, as can be roughly estimated from Figure 2a. Considering a nominal spacing of the docking nanodots equal to 60 nm and assuming that in order to self-limit docking *via* steric hindrance, the nanodots and nanodumbbell tips should have a similar size (*i.e.*, d_d = 2 nm), then the nanodumbbell length must be kept between 54 and 62 nm. To verify this, we synthesized nanodumbbells that fit this requirement (see Supporting Information, Figure S2). We measured the length distribution based on transmission electron microscopy (TEM) imaging and found that 82% of the nanodumbbells fall within the length range of 54 and 62 nm. This implies that although most of the nanodumbbells would, in principle, dock with both of their edges, some could dock only with one edge. Therefore, even if the extreme miniaturization of nanodots is technically possible, there will always be a trade-off between the steric hindrance that minimizes multiple docking and the yield of the assembly. Alternatively, minimizing multiple docking while keeping a high yield of assembly is possible by enlarging the nanodumbbell tips to 6–7 nm.[48,49] Also, some of the nanodumbbells might have a Au tip on only one edge, because of the imperfect yield of the tip growth process. This little constraint, which is only relevant to the case of double docking, should be addressed by optimizing the conditions of tip growth, aiming at maximizing its yield.

DOI: 10.1021/acsnano.8b04443
ACS Nano XXXX, XXX, XXX–XXX

CONCLUSIONS

In summary, we demonstrated a strategy for the controlled organization of inorganic quasi-1D nanostructures *via* chemical docking of their tips to nanopatterned functionalities. Notably, various methods for the directed assembly were proposed for vapor-phase-grown 1D nanostructures with micrometer-scale length and width of at least several tens of nanometers. Here, distinct quasi-1D inorganic nanostructures with sub-10 nm diameter and sub-100 nm length were controllably positioned with such precision and in a parallel manner. This precision was achieved by using sub-10 nm docking nanofunctionalities and is unlikely achievable by other means. We fabricated the docking nanodot arrays by nanoimprint lithography, which provides the unique combination of a high throughput, scalability, pattern arbitrariness, and sub-10 nm feature size. Thus, nanoimprint lithography is ideal for the fabrication of functional arrays that encode the assembly of distinct nanodumbbells.

We have shown that the docking of Au nanodumbbell tips to metallic nanodots is possible using organic dithiols. This is probably the simplest and most straightforward strategy to chemically bridge two surfaces, but it is not the only one. Site-specific binding of a nano-object was previously demonstrated through various interactions, such as electrostatic attraction,[48−50] chemical recognition,[51] and DNA folding.[30] We believe that these strategies can also be applied to nanodumbbell docking, and we intend to explore them in the future. We demonstrated that multiple nanodumbbells can dock to 5−10 nm nanodots. We believe that miniaturizing nanodot dimensions to the size of the nanodumbbell tips could minimize multiple docking. The ability to spatially arrange liquid-synthesized 1D nanostructures in a programmable manner with nanoscale precision, arbitrary geometry, and long-range order enables exploiting their unique physical properties by integrating them into functional nanodevices and nanocircuits. In addition to pushing the boundaries of nanodevice miniaturization, this strategy can potentially facilitate bottom-up realization of nanosystems with a structural and functional complexity unachievable nowadays.

MATERIALS AND METHODS

Materials. CdO (99.999%), *n*-hexylphosphonic acid (>97%), octadecylphosphonic acid (>97%), trioctylphosphine (>97%), trioctylphosphine oxide (99%), and $AuCl_3$ (99%) were purchased from Strem Chemicals. Sulfur powder (99.98%), octadecene (99%), dodecylamine (98%), and didecyldimethylammonium bromide (98%) were purchased from Alfa Aesar.

Synthesis of Nanodumbbells. CdS−Au nanodumbbells were synthesized *via* a three-step seeded growth process. First, CdS quantum dots were synthesized. Then, theses dots were used as seeds for the growth of CdS nanorods followed by growth of Au tips, as described in a previous study.[22] See Supporting Information for a detailed description of the synthesis.

Nanopattern Fabrication. The fabrication was based on our previous work.[32] First, nanoimprint molds were produced using electron-beam lithography of hydrogen silsesquioxane (HSQ, XR-1541, Dow Corning). HSQ was diluted in methyl isobutyl ketone and spin-coated to produce a 20 nm thick film. The e-beam lithography was conducted in a Raith e-LINE with an acceleration voltage of 20 kV, aperture of 30 μm, and working distance of 10 mm. The samples were developed in AZ726 for 2 min, then immersed in distilled (DI) water and blow dried with nitrogen. The ready molds were annealed at 450 °C for 1 h and coated with a Nanonex NXT-110 antiadhesive agent. For the nanoimprint, Si samples were spin-coated with poly(methyl methacrylate) (PMMA) (50K, Microchem) and baked on a hot plate heated to 180 °C for 2 min. The PMMA thickness was 40 nm. The imprint was done at 450 psi, 180 °C, for 4 min using a Nanonex NX-B100 nanoimprinter. A Ti mask of ∼10 nm was evaporated at an angle of 60° in an electron-beam evaporator. The samples were etched with deep reactive ion etching (Corial 200 IL) using oxygen plasma. Then, Ti/AuPd (1 nm/3 nm) film was evaporated perpendicularly to the samples. Lift-off was done by sonicating the samples in acetone. Finally, the samples were annealed for 1 h at 550 °C under a N_2 atmosphere.

Functionalization. The arrays were cleaned by immersion for 10 min in piranha solution that was aged for 3 h beforehand, rinsed with DI water, and then cleaned in oxygen plasma (Harrick PDC-32G, 1 min). Immediately after the plasma treatment, samples were immersed in a 5 mM ethanolic solution of 1,6-hexanedithiol and left under gentle agitation overnight. The samples were cleaned by replacing the dithiol solution with fresh ethanol, sonicating for 5 min, rinsing in ethanol, and blow drying with nitrogen.

Docking. Vials containing nanodumbbells in toluene were prepared prior to the end of the functionalization process. The functionalized substrates were immersed in the solution and placed on a shaker. Importantly, the vessel with the nanodumbbell solution was kept closed and sealed during the process, to prevent toluene evaporation and keep the nanodumbbell concentration constant. Docking was performed at varied concentrations and times (see Supporting Information for assessment of nanodumbbell concentration). At the end of the assembly process, the samples were cleaned by replacing the liquid in the vial with fresh toluene, then rinsing with toluene and blow drying with nitrogen.

Characterization. After the docking, samples were characterized by SEM. The analysis was performed by counting the number of occurrences of sites containing the same amount of nanodumbbells (number of docking sites with 0, 1, 2, ... nanodumbbells). Probability was calculated by dividing the number of occurrences for each amount by the total number of occurrences. The obtained numbers of nanodumbbells (D) and docking sites (N) were used in the model according to eq 1 for each amount of nanodumbbells per site (A).

ASSOCIATED CONTENT

Supporting Information

The Supporting Information is available free of charge on the ACS Publications website at DOI: 10.1021/acsnano.8b04443.

> Nanodumbbell synthesis; pattern fabrication scheme; concentration assessment method; length distribution method; random attachment model derivation and schematic size discrepancy tolerance for docking (PDF)

AUTHOR INFORMATION

Corresponding Authors

*E-mail: mokari@bgu.ac.il.
*E-mail: marksc@bgu.ac.il.

ORCID

Avichai Marcovici: 0000-0003-3266-3661
Guillaume Le Saux: 0000-0003-4902-1980
Mark Schvartzman: 0000-0002-5912-525X

Notes

The authors declare no competing financial interest.

ACKNOWLEDGMENTS

This work was funded by the Israel Science Foundation, Individual Grant # 1401/15 to T.M.

DOI: 10.1021/acsnano.8b04443
ACS Nano XXXX, XXX, XXX−XXX

REFERENCES

(1) Trudeau, P. E.; Sheldon, M.; Altoe, V.; Alivisatos, A. P. Electrical Contacts to Individual Colloidal Semiconductor Nanorods. *Nano Lett.* **2008**, *8*, 1936−1939.

(2) Gudiksen, M. S.; Maher, K. N.; Ouyang, L.; Park, H. Electroluminescence from a Single-Nanocrystal Transistor. *Nano Lett.* **2005**, *5*, 2257−2262.

(3) Kazes, M.; Lewis, D. Y.; Ebenstein, Y.; Mokari, T.; Banin, U. Lasing from Semiconductor Quantum Rods in a Cylindrical Microcavity. *Adv. Mater.* **2002**, *14*, 317−321.

(4) Huynh, W. U. Hybrid Nanorod-Polymer Solar Cells. *Science* **2002**, *295*, 2425−2427.

(5) Xia, Y.; Yang, P.; Sun, Y.; Wu, Y.; Mayers, B.; Gates, B.; Yin, Y.; Kim, F.; Yan, H. One-Dimensional Nanostructures: Synthesis, Characterization, and Applications. *Adv. Mater.* **2003**, *15*, 353−389.

(6) Weber, J.; Singhal, R.; Zekri, S.; Kumar, A. One-Dimensional Nanostructures: Fabrication, Characterization and Applications. *Int. Mater. Rev.* **2008**, *53*, 235−255.

(7) Lu, W.; Xiang, J.; Timko, B. P.; Wu, Y.; Lieber, C. M. One-Dimensional Hole Gas in Germanium/Silicon Nanowire Heterostructures. *Proc. Natl. Acad. Sci. U. S. A.* **2005**, *102*, 10046−10051.

(8) Whitesides, G. M.; Grzybowski, B. Self-Assembly at All Scales. *Science* **2002**, *295*, 2418−2421.

(9) Huang, Y.; Duan, X. F.; Wei, Q. Q.; Lieber, C. M. Directed Assembly of One-Dimensional Nanostructures into Functional Networks. *Science* **2001**, *291*, 630−633.

(10) Fan, Z.; Ho, J. C.; Jacobson, Z. A.; Yerushalmi, R.; Alley, R. L.; Razavi, H.; Javey, A. Wafer-Scale Assembly of Highly Ordered Semiconductor Nanowire Arrays by Contact Printing. *Nano Lett.* **2008**, *8*, 20−25.

(11) Yao, J.; Yan, H.; Lieber, C. M. A Nanoscale Combing Technique for the Large-Scale Assembly of Highly Aligned Nanowires. *Nat. Nanotechnol.* **2013**, *8*, 329−335.

(12) Freer, E. M.; Grachev, O.; Duan, X.; Martin, S.; Stumbo, D. P. High-Yield Self-Limiting Single-Nanowire Assembly with Dielectrophoresis. *Nat. Nanotechnol.* **2010**, *5*, 525−530.

(13) Tsivion, D.; Schvartzman, M.; Popovitz-Biro, R.; von Huth, P.; Joselevich, E. Guided Growth of Millimeter-Long Horizontal Nanowires with Controlled Orientations. *Science* **2011**, *333*, 1003−1007.

(14) Schvartzman, M.; Tsivion, D.; Mahalu, D.; Raslin, O.; Joselevich, E. Self-Integration of Nanowires into Circuits *via* Guided Growth. *Proc. Natl. Acad. Sci. U. S. A.* **2013**, *110*, 15195−15200.

(15) Yin, Y.; Alivisatos, P. A. Colloidal Nanocrystal Synthesis and the Organic-Inorganic Interface. *Nature* **2005**, *437*, 664−670.

(16) Manna, L.; Scher, E.; Alivisatos, A. P. Synthesis of Soluble and Processable Rod-,Arrow-, Teardrop-, and Tetrapod-Shaped CdSe Nanocrystals. *J. Am. Chem. Soc.* **2000**, *122*, 12700−12706.

(17) Manfrinato, V. R.; Zhang, L.; Su, D.; Duan, H.; Hobbs, R. G.; Stach, E. A.; Berggren, K. K. Resolution Limits of Electron-Beam Lithography toward the Atomic Scale. *Nano Lett.* **2013**, *13*, 1555−1558.

(18) Chou, S. Y.; Krauss, P. R.; Renstrom, P. J. Imprint Lithography with 25-Nanometer Resolution. *Science* **1996**, *272*, 85−87.

(19) Glass, R.; Muller, M.; Spatz, J. P. Block Copolymer Micelle Nanolithography. *Nanotechnology* **2003**, *14*, 1153−1160.

(20) Ding, B.; Wu, H.; Xu, W.; Zhao, Z.; Liu, Y.; Yu, H.; Yan, H. Interconnecting Gold Islands with DNA Origami Nanotubes. *Nano Lett.* **2010**, *10*, 5065−5069.

(21) Penzo, E.; Palma, M.; Wang, R.; Cai, H.; Zheng, M.; Wind, S. J. Directed Assembly of End-Functionalized Single Wall Carbon Nanotube Segments. *Nano Lett.* **2015**, *15*, 6547−6552.

(22) Mokari, T.; Rothenberg, E.; Popov, I.; Costi, R.; Banin, U. Selective Growth of Metal Tips Onto Semiconductor Quantum Rods and Tetrapods. *Science* **2004**, *304*, 1787−1790.

(23) Habas, S. E.; Yang, P.; Mokari, T. Selective Growth of Metal and Binary Metal Tips on CdS Nanorods. *J. Am. Chem. Soc.* **2008**, *130*, 3294−3295.

(24) Rukenstein, P.; Jen-La Plante, I.; Diab, M.; Chockler, E.; Flomin, K.; Moshofsky, B.; Mokari, T.; Alivisatos, A. P.; Cingolani, R.; Manna, L. Selective Growth of Metal Sulfide Tips onto Cadmium Chalcogenide Nanostructures. *CrystEngComm* **2012**, *14*, 7590−7593.

(25) Ji, B.; Panfil, Y. E.; Banin, U. Heavy-Metal-Free Fluorescent ZnTe/ZnSe Nanodumbbells. *ACS Nano* **2017**, *11*, 7312−7320.

(26) Mokari, T.; Sztrum, C. G.; Salant, A.; Rabani, E.; Banin, U. Formation of Asymmetric One-Sided Metal-Tipped Semiconductor Nanocrystal Dots and Rods. *Nat. Mater.* **2005**, *4*, 855−863.

(27) Rukenstein, P.; Teitelboim, A.; Volokh, M.; Diab, M.; Oron, D.; Mokari, T. Charge Transfer Dynamics in CdS and CdSe@CdS Based Hybrid Nanorods Tipped with Both PbS and Pt. *J. Phys. Chem. C* **2016**, *120*, 15453−15459.

(28) Wu, W.; Tong, W. M.; Bartman, J.; Chen, Y.; Walmsley, R.; Yu, Z.; Xia, Q.; Park, I.; Picciotto, C.; Gao, J.; Wang, S. Y.; Morecroft, D.; Yang, J.; Berggren, K. K.; Williams, R. S. Sub-10 Nm Nanoimprint Lithography by Wafer Bowing. *Nano Lett.* **2008**, *8*, 3865−3869.

(29) Ahn, S. H.; Guo, L. J. Large-Area Roll-to-Roll and Roll-to-Plate Nanoimprint Lithography: A Step toward High-Throughput Application of Continuous Nanoimprinting. *ACS Nano* **2009**, *3*, 2304−2310.

(30) Lalander, C. H.; Zheng, Y.; Dhuey, S.; Cabrini, S.; Bach, U. DNA-Directed Self-Assembly of Gold Nanoparticles onto Nanopatterned Surfaces: Controlled Placement of Individual Nanoparticles into Regular Arrays. *ACS Nano* **2010**, *4*, 6153−6161.

(31) Pearson, A. C.; Pound, E.; Woolley, A. T.; Linford, M. R.; Harb, J. N.; Davis, R. C. Chemical Alignment of DNA Origami to Block Copolymer Patterned Arrays of 5 Nm Gold Nanoparticles. *Nano Lett.* **2011**, *11*, 1981−1987.

(32) Schvartzman, M.; Wind, S. J. Robust Pattern Transfer of Nanoimprinted Features for Sub-5-Nm Fabrication. *Nano Lett.* **2009**, *9*, 3629−3634.

(33) Schvartzman, M.; Palma, M.; Sable, J.; Abramson, J.; Hu, X.; Sheetz, M. P.; Wind, S. J. Nanolithographic Control of the Spatial Organization of Cellular Adhesion Receptors at the Single-Molecule Level. *Nano Lett.* **2011**, *11*, 1306−1312.

(34) Cai, H.; Depoil, D.; Palma, M.; Sheetz, M. P.; Dustin, M. L.; Wind, S. J. Bifunctional Nanoarrays for Probing the Immune Response at the Single-Molecule Level. *J. Vac. Sci. Technol., B: Nanotechnol. Microelectron.: Mater., Process., Meas., Phenom.* **2013**, *31*, 06F902.

(35) Cherniavskaya, O.; Chen, C. J.; Heller, E.; Sun, E.; Provezano, J.; Kam, L.; Hone, J.; Sheetz, M. P.; Wind, S. J. Fabrication and Surface Chemistry of Nanoscale Bioarrays Designed for the Study of Cytoskeletal Protein Binding Interactions and Their Effect on Cell Motility. *J. Vac. Sci. Technol., B: Microelectron. Process. Phenom.* **2005**, *23*, 2972.

(36) Vericat, C.; Vela, M. E.; Benitez, G.; Carro, P.; Salvarezza, R. C. Self-Assembled Monolayers of Thiols and Dithiols on Gold: New Challenges for a Well-Known System. *Chem. Soc. Rev.* **2010**, *39*, 1805−1834.

(37) Talapin, D. V.; Shevchenko, E. V.; Murray, C. B.; Kornowski, A.; Föraster, S.; Weller, H. CdSe and CdSe/CdS Nanorod Solids. *J. Am. Chem. Soc.* **2004**, *126*, 12984−12988.

(38) Bunge, S. D.; Krueger, K. M.; Boyle, T. J.; Rodriguez, M. A.; Headley, T. J.; Colvin, V. L. Growth and Morphology of Cadmium Chalcogenides: The Synthesis of Nanorods, Tetrapods, and Spheres from CdO and Cd(O2CCH3)2. *J. Mater. Chem.* **2003**, *13*, 1705−1709.

(39) Yang, P.; Kim, F. Langmuir-Blodgett Assembly of One-Dimensional Nanostructures. *ChemPhysChem* **2002**, *3*, 503−506.

(40) Ghezelbash, A.; Koo, B.; Korgel, B. A. Self-Assembled Stripe Patterns of CdS Nanorods. *Nano Lett.* **2006**, *6*, 1832−1836.

(41) McCarley, R. L.; Dunaway, D. J.; Willicut, R. J. Mobility of the Alkanethiol-Gold(111) Interface Studied by Scanning Probe Microscopy. *Langmuir* **1993**, *9*, 2775−2777.

(42) Sheldon, M. T.; Trudeau, P. E.; Mokari, T.; Wang, L. W.; Paul Alivisatos, A. Enhanced Semiconductor Nanocrystal Conductance *via* Solution Grown Contacts. *Nano Lett.* **2009**, *9*, 3676−3682.

DOI: 10.1021/acsnano.8b04443
ACS Nano XXXX, XXX, XXX−XXX

(43) Salant, A.; Amitay-Sadovsky, E.; Banin, U. Directed Self-Assembly of Gold-Tipped CdSe Nanorods. *J. Am. Chem. Soc.* **2006**, *128*, 10006−10007.
(44) Piran, U.; Riordan, W. J. Dissociation Rate Constant of the Biotin-Streptavidin Complex. *J. Immunol. Methods* **1990**, *133*, 141−143.
(45) Penzo, E.; Wang, R.; Palma, M.; Wind, S. J. Selective Placement of DNA Origami on Substrates Patterned by Nanoimprint Lithography. *J. Vac. Sci. Technol., B: Nanotechnol. Microelectron.: Mater., Process., Meas., Phenom.* **2011**, *29*, 06F205.
(46) Adamczyk, Z.; Jaszczółt, K.; Michna, A.; Siwek, B.; Szyk-Warszyńska, L.; Zembala, M. Irreversible Adsorption of Particles on Heterogeneous Surfaces. *Adv. Colloid Interface Sci.* **2005**, *118*, 25−42.
(47) Javey, A.; Dai, H. Regular Arrays of 2 Nm Metal Nanoparticles for Deterministic Synthesis of Nanomaterials. *J. Am. Chem. Soc.* **2005**, *127*, 11942−11943.
(48) Nidetz, R.; Kim, J. Directed Self-Assembly of Nanogold Using a Chemically Modified Nanopatterned Surface. *Nanotechnology* **2012**, *23*, 045602.
(49) Gilles, S.; Kaulen, C.; Pabst, M.; Simon, U.; Offenhäusser, A.; Mayer, D. Patterned Self-Assembly of Gold Nanoparticles on Chemical Templates Fabricated by Soft UV Nanoimprint Lithography. *Nanotechnology* **2011**, *22*, 295301.
(50) He, H. X.; Zhang, H.; Li, Q. G.; Zhu, T.; Li, S. F. Y.; Liu, Z. F. Fabrication of Designed Architectures of Au Nanoparticles on Solid Substrate with Printed Self-Assembled Monolayers as Templates. *Langmuir* **2000**, *16*, 3846−3851.
(51) Abramson, J.; Palma, M.; Wind, S. J.; Hone, J. Quantum Dot Nanoarrays: Self-Assembly with Single-Particle Control and Resolution. *Adv. Mater.* **2012**, *24*, 2207−2211.

DOI: 10.1021/acsnano.8b04443
ACS Nano XXXX, XXX, XXX−XXX